# Phase-reference mapping of nearby stars: status report

W. Alef (MPIfR, Bonn)
A. Benz (ETH, Zürich)
J. Conway, M. Pestalozzi (Onsala)
T. Beasley (NRAO, Charlottesville)

**Abstract**

We have observed radio emitting stars in phase-referenced mode with both the VLBA and the EVN in order to map their brightness distributions and to determine precise astrometric parameters. While the VLBA correlator uses the CALC 8 model, the older MK3 correlator model is not sufficient to make phase-referenced mapping possible using the visibility amplitude and residual phase. In the raw MK3 correlated data we have successfully replaced the correlator model with the CALC 8 model. We have shown that phase-reference mapping is possible with MK3 data for source separations of 2 to 3 degrees. At present we are exploring the possibility of removing ionospheric and atmospheric contributions, which are not modelled at all in CALC 8, and which decrease the SNR in phase-reference maps in general by a factor of 2 to 3.

## 1 Introduction

Standard VLBI observing techniques are sensitivity-limited to radio sources whose correlated flux can be detected by integration within the time interval for which the interferometer can be regarded as phase-stable. This time — the coherence time — ranges from a few seconds for the highest and lowest observing frequencies used in VLBI to 20 minutes and more for intermediate frequencies under favourable conditions. Another drawback of the standard methods is that the so-called phase self-calibration algorithms remove all astrometric information contained in the data.

The coherence of a VLBI interferometer can be extended by calibrating the phase instabilities. This is achieved by switching between the target and a nearby strong phase-calibrator on time scales shorter than the coherence time. At the same time absolute relative astrometric information can be retained (relative to the calibrator). This method is called phase-referencing. When used to map (weak) radio sources directly, we speak of phase-reference mapping, and the image of the observed object is recovered by Fourier-transforming[1] all the phase-calibrated data from the (u,v)- to the image-plane and subsequent de-convolution.

For astronomical VLBI observers it is very desirable if the production of phase-referenced images can be done within the framework of the most widely used astronomical data reduction and mapping software AIPS (Greisen, 1990) which is also used for reducing standard VLBI observations.

In AIPS nearly all programs that are needed for phase-reference mapping are already available. All of the data manipulation is done on the residual correlated data. The disadvantage of this approach is that bad correlator models like that used in MK3 correlators, or errors in the a priori interferometer geometry can lead to de-correlation in the phase-referenced image (see Fig. 1) such that the flux of the source to be mapped is spread around in the image so that the target cannot be detected anymore as it is swamped by the increased noise. In addition changes in the correlator model can make astrometric comparisons between different observing epochs difficult or even impossible.

To overcome the above mentioned problems one of us has written an AIPS task which allows to change the correlator model after the correlation (Beasley & Alef, 1998).

[1]The Fourier-transformation vector sums all the (u,v)-data, with a different phase gradient applied for each point in the image plane

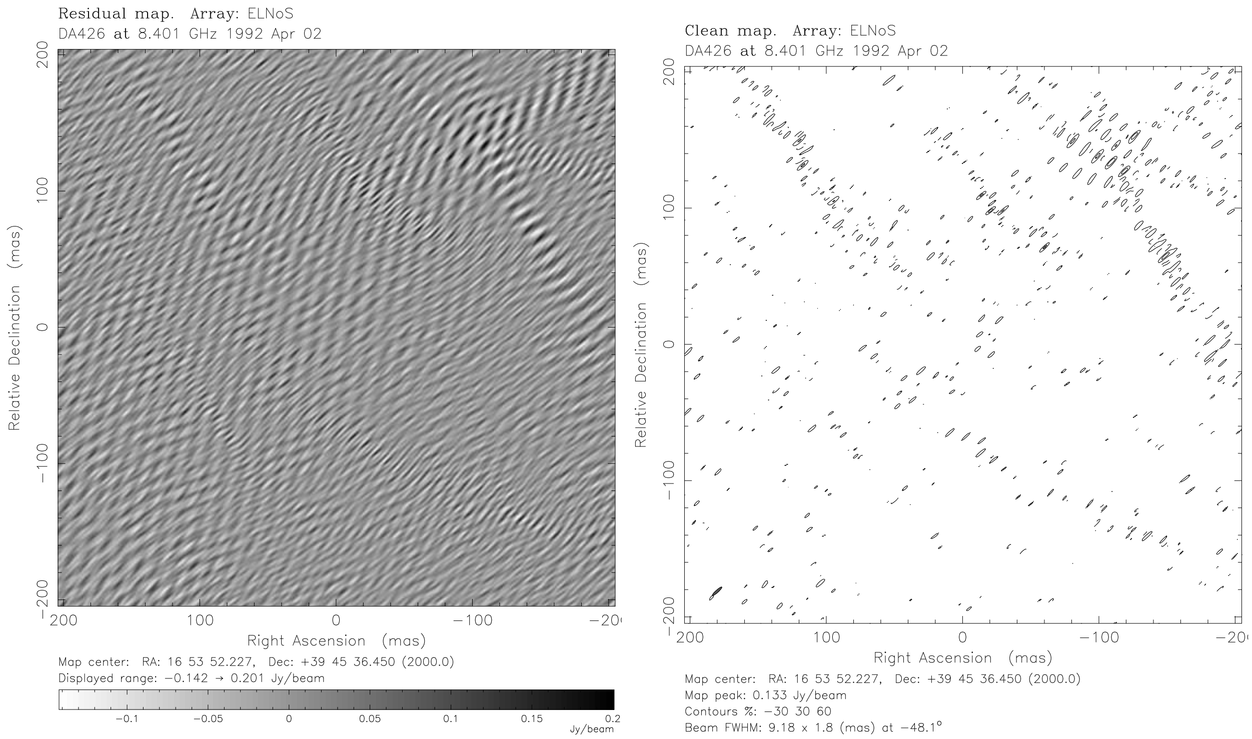


*Fig. 1: The left picture shows the dirty (not de-convolved) image of the test target source. The right picture shows the same image, but de-convolved. The source flux appears spread in a wide area in the upper right corner of the images. This is due to errors in the interferometer geometry and a simplistic correlator model.*

## 2 Observations

There is an increasing desire to extend the high-resolution studies of radio sources to objects with lower flux, which cannot be investigated anymore with the standard methods of VLBI interferometry. Our group is studying the radio emission from dwarf stars of spectral type M (dMe; Gary and Linsky, 1981), which produce emission from occasional flares as well as the persistent, low-level, slowly variable 'quiescent' component. Typical fluxes range from a few tens of mJy during flares down to about 1 mJy for the quiescent phases. Our main aim is to gain more understanding of the emission processes. Eventually we would like to make a radio image of suitable stars whose size matches the resolution properties of the available arrays. The most difficult and challenging project requires high precision astrometry: search for "small" planets orbiting at a few AU around nearby stars. With optimistic assumptions we should be able to detect a planet of 0.1 Jupiter mass circling a star with 0.3 $M_{\odot}$ at a distance of 5 pc.

So far our group has observed five different stars with typical fluxes around 1 mJy. We used both the VLBA supplemented by the high sensitivity of the tied VLA array, and the EVN (Effelsberg, Medicina, Noto, Onsala, Shanghai, Urumqi) together with telescopes of the geodetic network (Crimea, Madrid, Matera, South Africa, Wettzell). The observations were done at 8.4 GHz. The recording bit rates were 128 and 112 Mbit/s (Mode A) respectively. In all cases the telescopes switched back and forth between the star and a strong compact radio source — the phase calibrator — within 5 minutes in order to track the phase instabilities. The separation of target and reference was in all cases about 2° to 3°.

The theoretical 1 $\sigma$ image noise limit for both arrays for a full track and about five hours net data on the target is about 50 $\mu$Jy. For a reliable detection of a point source we need about 10 $\sigma$. Thus we should be able to detect point sources as weak as 500 $\mu$Jy.

Not all of the EVN observations were successful, e.g. incompatibilities between geodetic and astronomical setups for the VC to IF patching (has to be done by hand) caused data loss. A hardware failure of the Effelsberg telescope made a complete observation worthless.

## 3 Software Development

All of the post-correlation data reduction was done in AIPS using the residuals to the correlator model. The data reduction path was as follows:

1. The raw correlated data was loaded from DATs. For VLBA data the AIPS task FITLD is used while MK3 data is read in with MK3IN. The VLBA correlator produces data in the cross-spectral domain with an antenna-based model stored with the data. MK3IN transforms the data from a baseline- and lag-based MK3 correlator to the cross-spectral domain and recovers an antenna-based correlator model from the baseline-based information in the data. After this initial step the data set is a file with all the raw correlation coefficients with weights (formal errors) and a set of tables with source, antenna, frequency, flag, and scan information, a calibration table which is filled and modified in the following steps, and maybe a table with the correlator model.

2. Phase-cal phases, parallactic angle corrections, and amplitude calibration were applied (stored in the calibration table). Data known to be bad were flagged.

3. The data of the phase-calibrator were fringe fitted with the antenna-based fitting task FRING. The structure phase of both sources is still contained in the data.

4. The resulting phase and delay measured on the calibrator were interpolated over the gaps in which the target source was observed. The phase ambiguities were resolved by using the fringe rates. Resulting values for the target source were stored in the calibration table

5. The data were split into a file per source and the calibration table is applied to the data of both the reference and the target, which scales the amplitudes and subtracts the (time-dependent) instrumental phase from the visibility measurements.

6. The phase-calibrator was mapped with standard phase self-calibration techniques. Positional information for this source is lost.

7. The structure phase derived from the image of the phase-calibrator is transferred to the target source file and subtracted. The phase-center of the image is now the reference point for the relative position of the target source.

8. The data of the target source were resampled onto a regular (u,v) grid, it was inverted and deconvolved in the image plane. The resulting phase-referenced image shows (assuming sufficient SNR) the true residual of the source positions used in the correlator model.

This worked well for VLBA data (with the above restrictions for inter-epoch comparisons). In order to make the above simple scheme feasible for MK3 data a new task PHREF was written which extracts the correlator model from the existing calibration table and replaces it with the CALC 8 model. This is reflected in a modified calibration table which has new calibration phases, rates and delays. After applying this table to the (u,v) data (step 5) the residual delays, rates and phases are equivalent to those that would have been produced using the VLBA correlator model. Station and source coordinates, clock parameters and time information are supplied via an external text file and can thus be different from the ones used at correlation time. This task has to be executed after step 1. The program was tested with short pieces of VLBA data with various errors in the interferometer geometry. The data corrected with PHREF was then compared to the same data correlated with the correct geometry. Some MK3 data correlated both at the Bonn MK3 correlator and at the VLBA correlator was used to test the MK3 mode of the program.
Known deficiencies are:

- The correction for the feed rotation of ALTAZ mounted antennas is not included in the CALC model and has to be applied with a different program.

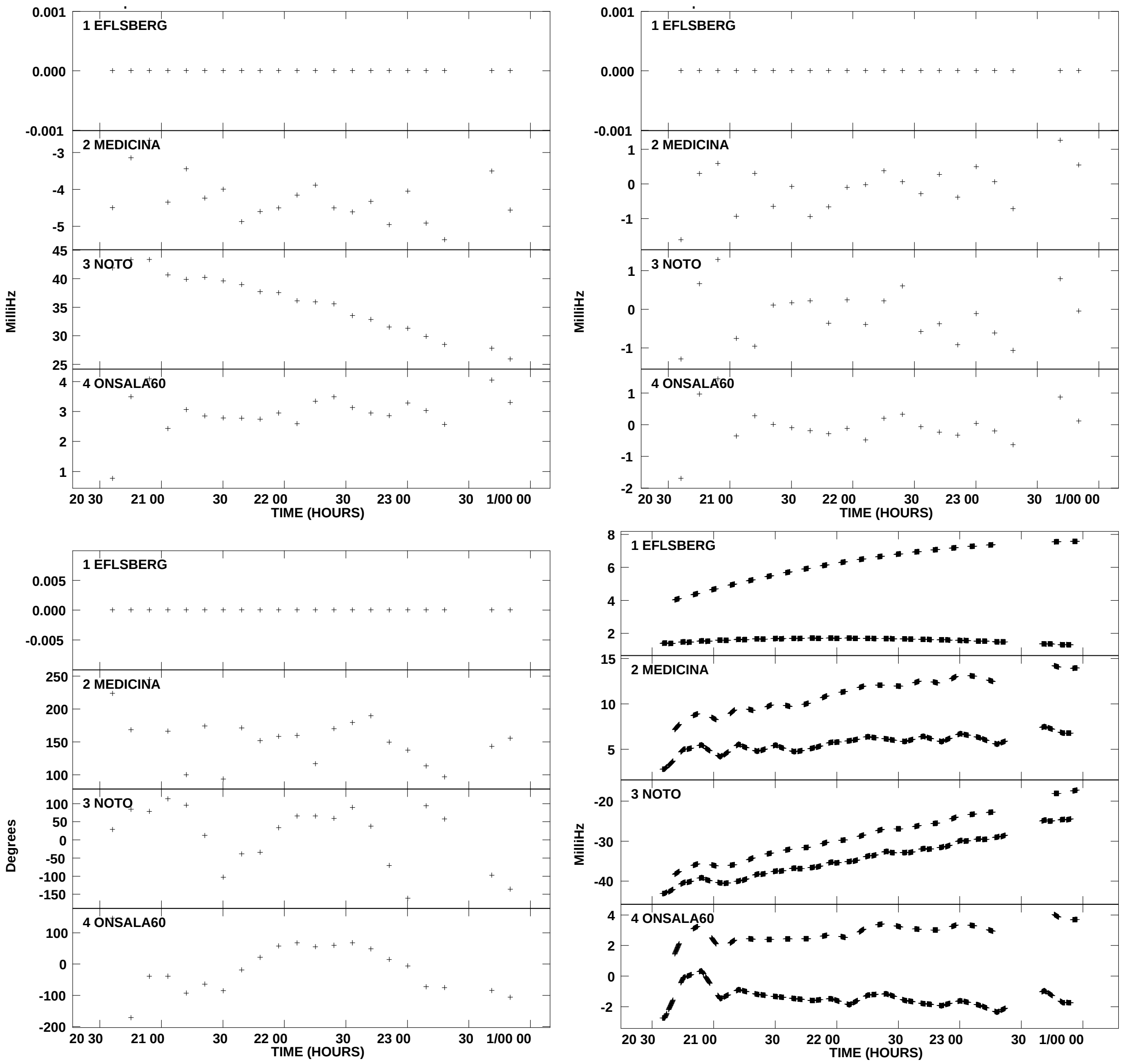


*Fig. 2: The figures show residuals per station as calculated by AIPS task FRING. Effelsberg was used as the reference station. Its residuals were arbitrarily set to 0. From left to right are shown: a) residual rate in mHz for uncorrected MK3 data, b) residual rate in mHz for MK3 data corrected by PHREF, c) residual phase in degrees of the corrected data, d) the total correction in fringe rate as estimated by PHREF + FRING residuals*

- No correction for ionospheric delay is possible at present, neither with measured values (e.g. GPS) nor with a model ionosphere.
- Only a station elevation dependant model of the dry atmosphere is used.
- Corrections for parallax are not implemented.
- Proper motion of stars cannot be taken into account. E.g. one star of our sample moves at 0.3 mas/h.

# 4 Results

We made further tests with MK3 data. A data set from a phase-referencing observation on two strong sources was analysed. As both a standard image and a phase-referenced image could be made, it was possible to verify how well the phase-reference mapping method works compared to the standard one.

A comparison of the fringe-fitting results of the calibrator (Fig. 2) shows that the original data has high residuals e.g. in fringe rate (Fig. 2a), while the corrected data gave residual fringe rates in a range of roughly $\pm 1.5$ mHz per antenna (Fig. 2b). The residual phases are slowly varying and can even be connected by eye (Fig. 2c). The total correction e.g. in fringe rate can be seen in Fig. 2d. The two lines correspond to the two observed sources for which we used slightly wrong positions at correlation time.
The calibrator source was mapped using the standard phase self-calibration method. It is point like and has structure phases of less than $\pm 5°$. Thus step 7 in the above recipe can be omitted. The data from the target source were calibrated with the interpolated rates, delays and phases. The corrected phase-referenced data was then interpolated onto a grid, Fourier-transformed and de-convolved.
The phase-referenced image with the corrected data (Fig. 3, left) is significantly better than the image made from the MK3 data without correcting the correlator model. By comparison with the standard image of the target source (Fig. 3, right) it becomes obvious though that the noise level is increased over the expected value; still a significant amount of flux is spread around in the image. The reason for this can be seen when the model phases are plotted against the phases which are corrected by the phase-referencing process (Fig. 4): on all baselines the measured and corrected phases scatter around the model by roughly $\pm 40°$. This scatter is significantly larger than the formal error of the phases as derived from the SNR. This scatter is a result of the interpolation of the calibration phase between scans of the reference source and application to the target at a distance of $2°$ to $3°$.

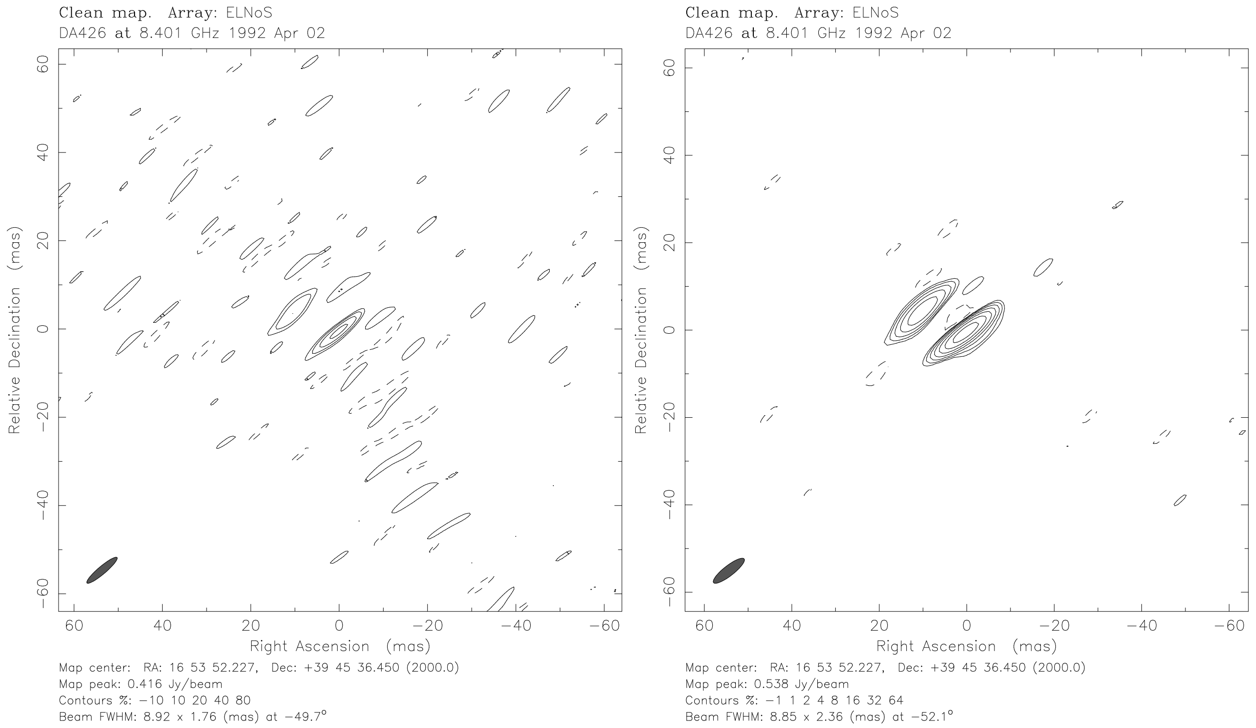


*Fig. 3: The left figure shows a phase-referenced image of the target. It is significantly better than the image shown in figure 2. The flux is now close to the image center. A few sidelobes due to the phase interpolation are visible and lead to an increased noise level. The figure on the right shows the same source mapped with the conventional phase self-calibration method. The noise level is significantly lower than in the phase-referenced image.*

It is a general finding that in phase-referenced images the recovered flux of the source is decreased while the noise in the image is increased. As a result the sensitivity is worse than the theoretical limit by roughly a factor of 2 to 3 as in this test case and other cases we (and other groups) investigated. Thus the theoretical limit for a detection of a point source is reduced from about 0.5 mJy to about 1.5 mJy.
While it is most likely that the loss of flux is due to temporal and spatial instabilities and effects not included in CALC 8 — mostly ionosphere and wet atmosphere — bugs in PHREF cannot be excluded

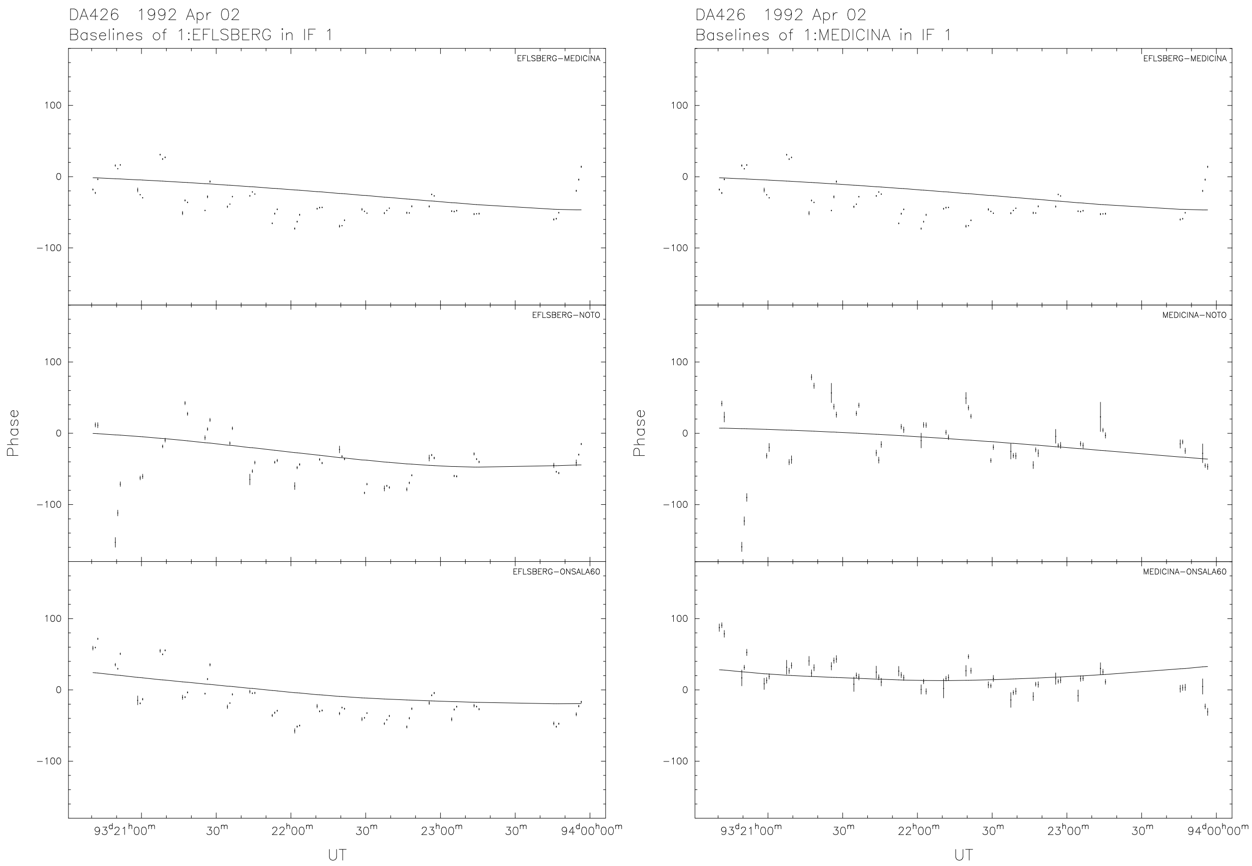


*Fig. 4: The phases on the baselines to Effelsberg (left) and Medicina (right) are shown. The model phase is indicated by the lines. The phase-referenced phases scatter around the model phase. This scatter disappears completely and the phases match the model if they are self-calibrated.*

completely (MK3 case). But any errors must be station and not baseline specific as self-calibrating the phase-connected data removes the phase scatter and recovers all of the flux. This means that if a source can be detected in a phase-referenced image, subsequent self-calibration will remove de-correlation in the image at the expense of astrometric precision. Similar results were found by other groups with VLBA data.

With our second test data set, L And was detected close to the fringe-fit signal-to-noise limit and thus could be mapped with both the traditional phase self-calibration and the phase-referencing methods, allowing us to compare the methods. We found significant de-correlation and in addition that structures seen in both images might not agree in the weak signal-to-noise domain (see Fig. 5). In the case of L And the image made directly with self-calibration is compatible with an unresolved point source, while the phase-reference image with subsequent self-calibration shows two roughly equal components. These two components are probably due to the side-lobe pattern in the phase-reference image which because of the low SNR could not be removed by the phase self-calibration.

# 5 Present and Future Work

A new AIPS task was written at NRAO to correct for the above mentioned effects of the path delay introduced by the ionosphere and its fluctuations. This task uses GPS measurements which are provided in IONEX format on various servers on the Internet. At present for the USA ionosphere images are available with a time spacing of 10 minutes, while for Europe the time intervals are still one hour. The new task undergoes extensive tests right now, but work by e.g. Ros, et al. (1999) has shown that GPS-based determinations of ionospheric delays can successfully be used for phase-referencing.

Correcting the delay due to the wet component of earth's atmosphere is significantly more difficult.

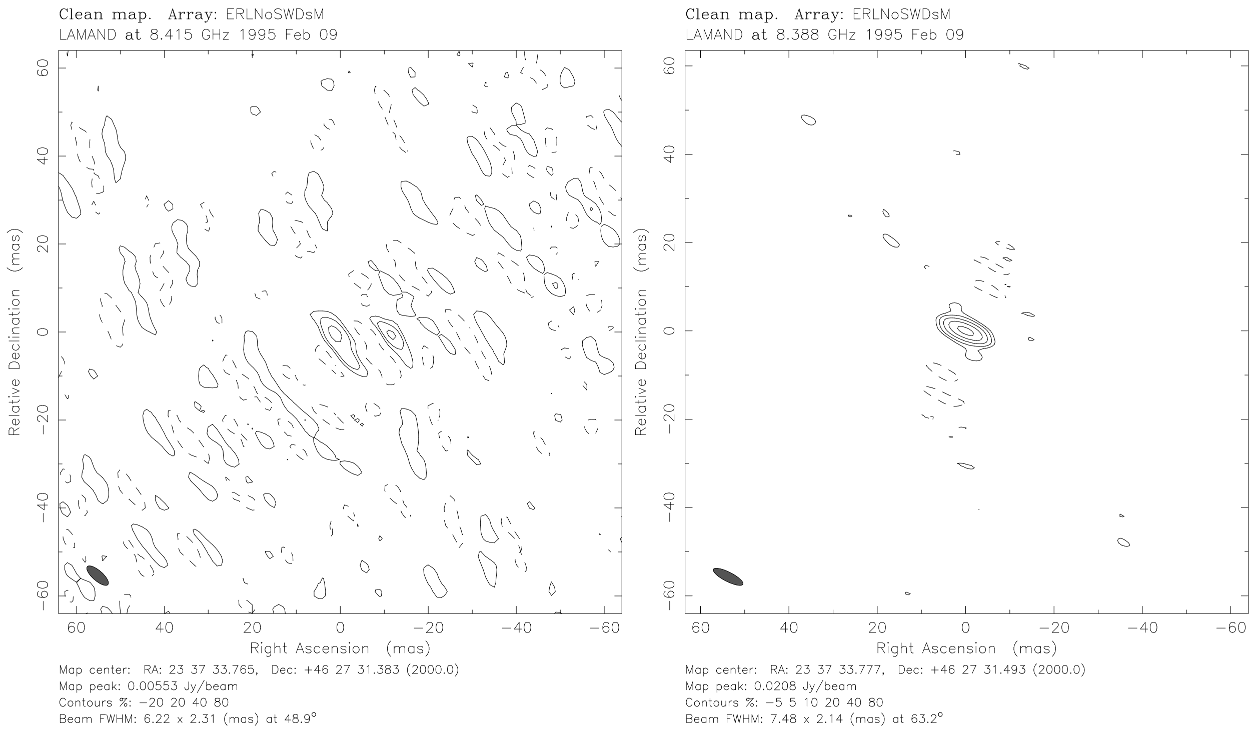


*Fig. 5: The figure on the left is a phase-referenced image of the star L And. It shows two components above the noise. If the data is in addition self-calibrated with this image the sidelobes are removed, but two components remain. The image on the right is a image of the same source made with standard phase self-calibration starting from a point source. It has only one unresolved component. This comparison shows that structures so close to the noise level are fairly unreliable.*

Tests with a task that uses ground-based measurements of pressure, humidity and temperature were only partly successful. This is due to the well-known fact that ground-based measurements may only describe the conditions in a thin layer over the telescope, while the wet delay is caused by a much thicker layer of the atmosphere. Possible improvements might be achieved by using water vapour radiometers or GPS measurements. A particularly interesting development is the new and very cheap (5000 $) water vapour radiometer designed at Haystack observatory.

A further reduction of systematic errors is expected when we have CALC 9 available. We plan to upgrade the above described task PHREF to CALC 9 as soon as possible. In particular the new CALC features of proper motion and parallax will be very useful for the observations of stars.

Another scheme which might be used to solve for ionospheric and atmospheric delays is being investigated: two strong reference sources are observed together with the target source. The net observing time on the target is reduced, but the two strong sources can be analysed and the residual differenced phase can be used to determine and model all unknown quantities (Ros, 1997).

After all these problems have been solved the astrometric precision might be high enough to allow us to measure displacements of nearby dwarf stars by earth-like planets, provided the radio emission is not significantly more extended than the star's surface.

# 6 Conclusions

We and other groups have shown that VLBI observations of stars and other weak radio sources are possible with the phase-reference mapping technique. To exploit the full potential of the method more work has to be invested to reduce the effects that cause de-correlation in the phase-referenced images. Once all the disturbing influences are under control it might be possible to achieve routine astrometric precision of position measurements relative to the phase-calibrator of about 0.1 mas for sources fluxes of about 1 mJy and over source separations of 2° to 3°.

# 7 References

Greisen E.W., 1990. "The Astronomical Image Processing System," in Acquisition, Processing and Archiving of Astronomical Images, eds. G. Longo and G. Sedmak, (Osservatorio Astronomico di Capodimonte and Centro di Formazione e studi per il Mezzogiorno), Naples, Italy.

Beasley A.J.; Alef W., 1998. Radio Emission from Galactic and Extragalactic Compact Sources, ASP Conference Series, Volume 144, IAU Colloquium 164, eds. J.A. Zensus, G.B. Taylor, & J.M. Wrobel, p. 405.

Gary D.E., Linsky J.L., 1981. ApJ 250,284

Ros E., Marcaide J.M., Guirado J.C., Sardón E., Shapiro I.I., "A GPS-based method to model the plasma effects in VLBI observations", 1999, A&A, inpreparation

Ros E., PhD Thesis, "Astrometria diferencial des precisión con VLBI en el Triánulo de Draco (y estudios de SN1993J)", Universitat de València, Spain, 1997.